Promoting extrinsic bridging of adhesively-bonded CFRP joints through the adhesive layer architecture

Tao, R.; Lubineau, Gilles; Teixeira De Freitas, S.

Publication date
2022

Document Version
Final published version

Published in
Proceedings of the 20th European Conference on Composite Materials: Composites Meet Sustainability

ECCM 20

26-30 JUNE 2022

LAUSANNE SWITZERLAND

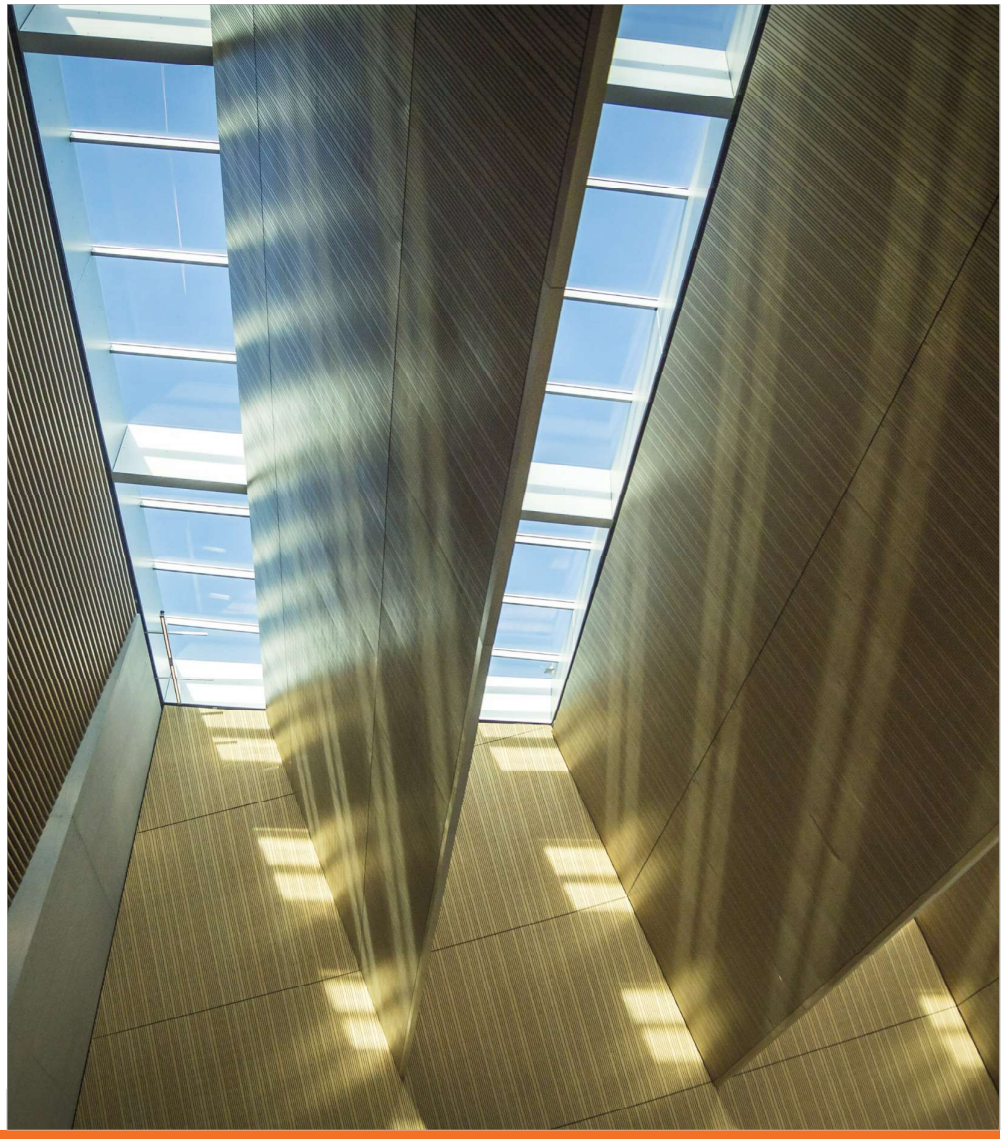

Proceedings of the 20th European Conference on Composite Materials

COMPOSITES MEET SUSTAINABILITY

Vol 2 – Manufacturing

Editors : Anastasios P. Vassilopoulos, Véronique Michaud

Organized by : EPFL CCLAB Composite Construction Laboratory

Under the patronage of : LPAC Laboratory for Processing of Advanced Composites; ESCM EUROPEAN SOCIETY FOR COMPOSITE MATERIALS

ECCM 20
26-30 JUNE 2022
LAUSANNE SWITZERLAND

EPFL CCLAB Composite Construction Laboratory LPAC Laboratory for Processing of Advanced Composites

Proceedings of the 20th European Conference on Composite Materials ECCM20 26-30 June 2022, EPFL Lausanne Switzerland

Edited By :

Prof. Anastasios P. Vassilopoulos, CCLab/EPFL
Prof. Véronique Michaud, LPAC/EPFL

Oragnized by:

Composite Construction Laboratory (CCLab)
Laboratory for Processing of Advanced Composites (LPAC)
Ecole Polytechnique Fédérale de Lausanne (EPFL)

ISBN: 978-2-9701614-0-0
DOI: http://dx.doi.org/10.5075/epfl-298799_978-2-9701614-0-0

Published by :

Composite Construction Laboratory (CCLab)
Ecole Polytechnique Fédérale de Lausanne (EPFL)
BP 2225 (Bâtiment BP), Station 16
1015, Lausanne, Switzerland

https://cclab.epfl.ch

Laboratory for Processing of Advanced Composites (LPAC)
Ecole Polytechnique Fédérale de Lausanne (EPFL)
MXG 139 (Bâtiment MXG), Station 12
1015, Lausanne, Switzerland

https://lpac.epfl.ch

Cover:

Swiss Tech Convention Center
© Edouard Venceslau - CompuWeb SA

Cover Design:

Composite Construction Laboratory (CCLab)
Ecole Polytechnique Fédérale de Lausanne (EPFL)
Lausanne, Switzerland

©2022 ECCM20/The publishers

Disclaimer:

Composites Meet Sustainability – Proceedings of the 20th European Conference on Composite Materials,
ECCM20. 26-30 June, 2022, Lausanne, Switzerland

PROMOTING EXTRINSIC BRIDGING OF ADHESIVELY-BONDED CFRP JOINTS THROUGH THE ADHESIVE LAYER ARCHITECTURE

Ran, Tao[a b], Gilles, Lubineau[a], Sofia, Teixeira De Freitas[b]

a: Mechanics of Composites For Energy and Mobility Lab, Mechanical Engineering Program, Physical Science and Engineering Division, King Abdullah University of Science and Technology (KAUST), Thuwal 23955-6900, Kingdom of Saudi Arabia
b: Structural Integrity & Composites, Faculty of Aerospace Engineering, Delft University of Technology, Delft, 2629 HS, the Netherlands
Presenter email: r.tao@tudelft.nl

Abstract: *Toughening and arresting crack propagation in secondary adhesive bonding of carbon fiber-reinforced polymers (CFRPs) are critical to their safety applications. Our previous work utilized the adhesive ligament bridging by alternatively patterning the mating surfaces, which successfully arrested the crack propagation under mode I loading. However, a large portion of the required energy is stored elastically in the stretching ligaments, which lead to sudden catastrophic debonding after the failure of ligaments. Two improvement methods are summarized in this work to further promote energy dissipation and slow down the catastrophic debonding. Integrating polyamide wires within the epoxy adhesive layer introduced complex failure mechanisms and bridging of embedded wires, while adopting a more ductile adhesive could largely extend the size of the bridging zone. Both methods are promising to soften the damage behavior when the bridging ligaments fail, and thus they both improve the reliability and damage tolerance of adhesively bonded joints.*

Keywords: CFRP; adhesive bonding; extrinsic bridging; wire reinforcement; mode I energy release rate;

1. Introduction

Carbon fiber-reinforced polymers (CFRPs) have widely attracted the aerospace and automotive industries due to high stiffness and lightweight. Secondary adhesive bonding of CFRPs is one of the most promising joining technologies to fully explore CFRP potential in full-scale structures where joints are inevitable. However, multiple challenges have limited the further application of adhesively-bonded composite joints since it is difficult to inspect the premature debonding, which leads to catastrophic failure once initiated. Thus, it is crucial to introduce crack arrest features, to slow down (or even stop) the crack growth and achieve progressive failure.

Various methods have been reported to introduce crack arrest features, including z-pins and corrugated substrates. Our previous work directly utilized the adhesive layer to bridge the separating CFRP parts, through the extrinsic bridging of adhesive ligaments [1]. The bridging adhesive ligaments are triggered by the patterning of distinct surface treatments. These extrinsic bridging ligaments largely enhance the energy release rate (ERR) and successfully arrest the crack propagation. However, due to the brittleness of the thermoset epoxy adhesive layer, the stored energy is released all at once after the failure of bridging ligaments, exaggerating the unstable crack propagation. Such safety concern will be elevated as the adhesive thickness increases, since more elastic energy will be stored, and then released, in thicker bridging

  doi:10.5075/epfl-298799_978-2-9701614-0-0

ligaments, which aligned with the analysis conducted in the previous work about the snap-back instability [2].

In this work, we modified the conventional brittle epoxy adhesive layer to further promote ERR and slow down the fast catastrophic crack propagation. By promoting the plastic energy dissipation, the bridging, stretching, and failure of generated adhesive ligaments could result in tougher and safer joints. To do so, two methods were summarized in this work. The first method is to integrate a ductile phase to the epoxy adhesive layer. In particular, various nylon (PA) wire structures were embedded into the epoxy adhesive layer and their effects on ERR were investigated experimentally under mode I double-cantilever beam (DCB) tests. The bonding CFRP substrates were alternatively patterned by two distinct surface treatments to achieve different interfacial strength and toughness values. The second method is to directly adopt an alternative adhesive material which exhibit a more ductile behavior, such as a methyl methacrylate adhesive (MMA) [3]. Numerical investigations were conducted to compare the influence of brittle epoxy and ductile methyl methacrylate adhesive (MMA) materials. Both experimental and numerical results showed that, with the alternative patterning surface treatment technique, a more ductile adhesive layer could further improve ERR and stabilize the crack propagation, leading to a toughened and safe adhesive joint.

2. Material and methods

2.1 Surface patterning on CFRP substrates

Unidirectional $[0]_8$ CFRP substrates (2 mm thick) were used in this work. Once cured, a surface patterning was applied to CFRP substrates, where the arrest interfaces, b=5 mm, were placed at a gap distance of 5 mm on top of the baseline interface, as shown in Figure 1. This type of patterning treatment on CFRP substrates aims to trigger adhesive ligaments during fracture tests, as already investigated in detail in our previous work [1]. In particular, in the experimental investigation for the first method, we used the pulsed CO_2 laser (PLS6.75 Laser Platform, Universal Laser Systems) to alternatively treat CFRP surfaces. Baseline interfaces were obtained using laser ablation (LA), which had pulse fluence of F_p=1.2 J/cm^2. While a lower fluence, F_p=0.4 J/cm^2, was deployed to slightly clean CFRP substrates (LC). LC regions feature better adhesion and therefore, so they were considered as arrest regions [4]. After laser-based patterning, CFRP substrates were immersed in acetone bath for a 10-min ultrasonic cleaning and then dried at 60°C in oven for 30 mins.

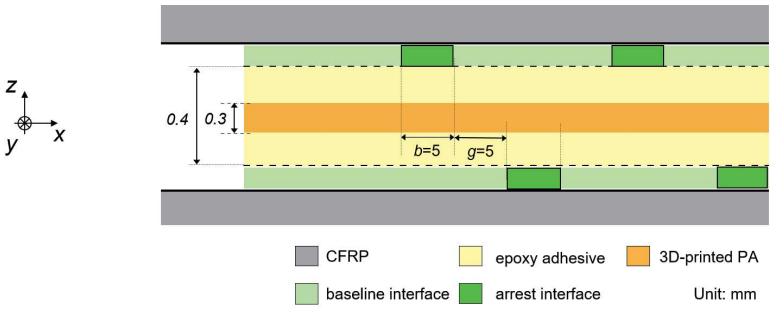

Figure 1. Schematic of the adhesive bonding with alternative patterning on CFRP substrates and 3D-printed PA wires (side view). The unit is mm in the schematic.

2.2 Integrating PA wires within epoxy adhesive

After the surface patterning, CFRP substrates were bonded using a hybrid adhesive layer, which consisted in a 3D printed PA structure embedded into an epoxy layer. The two-component epoxy adhesive was mixed at a weight ratio of 10:4 (resin versus hardener), and then it was applied to all CFRP substrate and PA surfaces to avoid voids. The PA wires were 3D-printed using fused filament fabrication. An example of 0.3-mm thick wire structure is shown in Figure 2 (a), where the printing was made along *x*-direction to ensure a high failure strength during the stretching. The adopted PA wires had a fixed width of 1 mm and three different spacing distances, as summarized in Table 1. As a comparison, we also tested a baseline configuration without inserting PA wires into the epoxy adhesive layer.

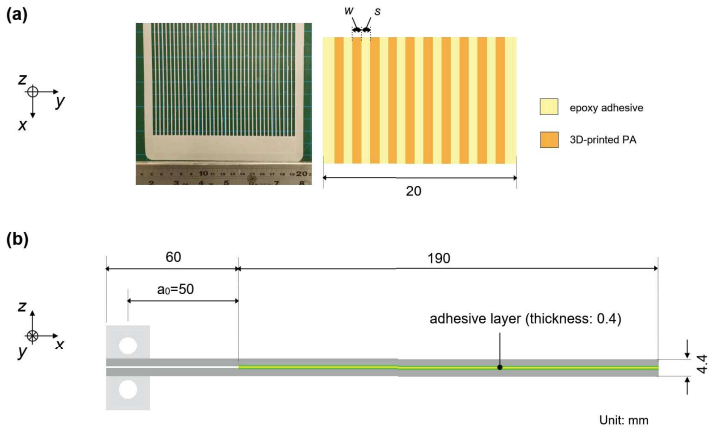

Figure 2. (a) Optical observation and schematic of 3D-printed PA wires. (b) Schematic of DCB specimen 20 mm wide. The unit is mm in the schematics.

Table 1: Three PA wires adopted in the work.

Batch	Wire width w [mm]	Spacing s [mm]	Wires per DCB sample [-]
wn2	1	9	2
wn5	1	3	5
wn10	1	1	10

2.3 Mode I fracture testing through DCB configurations

In order to evaluate the toughening effect resulting from the PA inserts, mode I fracture tests were carried out using the DCB configuration. To introduce a pre-crack, a non-sticky polyethylene (60-mm long) was positioned between the bonding of the two treated substrates. The DCB specimens were in the vacuum-oven under 60°C for 3 hours with a mechanical pressure to ensure a full adhesive-CFRP contact. The curing temperature was selected based on the thermal properties characterized in our previous work to achieve a good PA-epoxy interaction and avoid PA discoloration [5]. The thickness of the entire adhesive layer was controlled to be 0.4 mm. After curing, we cut the bonded plate into a size of 250x20 mm^2, following the

recommendations of ASTM D5528-13 standard [6]. At last, aluminum loading blocks were bonded to the specimens to apply the end peel loading by a universal testing machine (Instron 5882, Instron, Massachusetts, USA), as shown in the schematic in Figure 2 (b).

Six DCB specimens were tested for each configuration under the displacement control at a rate of 0.5 mm/min. On the side of each DCB specimen, we manually drew a scale to identify the crack propagation length, which was recorded through a high-resolution camera. The energy release rate (ERR, G_I) was obtained to analyze the failure mechanisms of the integrated PA structures. In this work, the compliance calibration (CC) data reduction method was used to determine ERR [6].

2.4 2D FEM simulation of brittle and ductile adhesive material

To compare two different adhesive material properties, 2D finite element (FE) simulations were performed using a DCB configuration, shown in Figure 3 (a). In this model, the unidirectional CFRP substrates were 1 mm thick with the following orthotropic properties based on the datasheet of Hexply 8552 AS4: E_x=141 GPa, E_y=E_z=10 GPa, G_{xy}=G_{xz}=3.3 GPa, G_{yz}=3.6 GPa, ν_{xy}= ν_{xz}=0.3, and ν_{yz}=0.38. Three different thickness values of the adhesive layer were modeled 0.5 mm, 1 mm, and 2 mm. Figure 3 (b) plots the Mises stress-strain curves adopted for the two distinct adhesive material types in [3]. It is clear that epoxy adhesive is brittle but has a higher strength, while MMA adhesive is much more ductile at the cost of lower strength. When both adhesives reach their strength values, the same damage behavior is assigned. Both the substrates and the adhesive were modeled using approximately 41000 2D plane strain elements CPE4R. The mesh convergence was validated in the previous work [7].

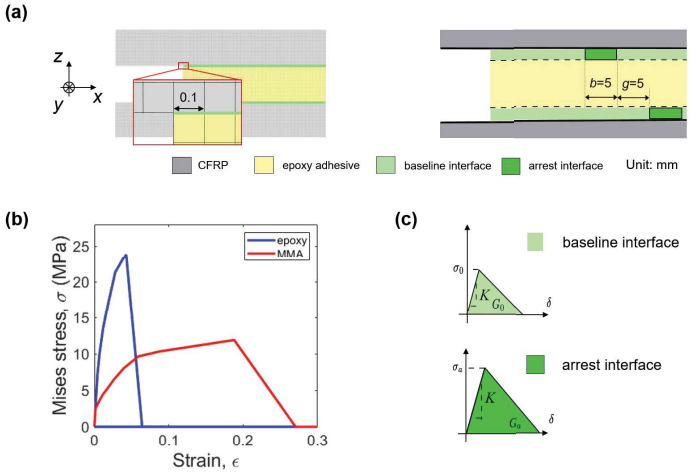

Figure 3. (a) Example of simulation mesh and schematics of DCB surface patterning (in mm). (b) Stress-strain curve of two adopted adhesive materials: brittle epoxy adhesive and ductile MMA adhesive. (c) Schematics of the traction-separation laws of baseline and arrest interfaces.

Similar to the experimental investigation, alternative patterning treatment was applied at the CFRP/adhesive interfaces, where two arrest interfaces were alternatively placed on the bottom and top baseline interfaces. The arrest size b is 5 mm and the gap between them is also 5 mm, as illustrated in Figure 3 (a). A bilinear traction-separation law was chosen for the two cohesive layers, which had 2200 COH2D4 elements (Figure 3 (c)). The baseline cohesive strength σ_0,

toughness G_0, arrest strength σ_a, and toughness G_a are based on the previous work [3], and the exact values are summarized in Table 2. Although mode I was the major fracture mode [7], the built-in quadratic traction-based criterion was employed to initiate the crack propagation. To stabilize the simulation when large load drop happens, a small viscosity value, 10^{-5}, was assigned to the cohesive element control [7]. An opening displacement was imposed on both loading blocks to simulate the opening load of the DCB testing, as indicated in Figure 3 (a).

Table 2: Interfacial properties of both configurations with epoxy and MMA adhesive materials.

Adhesive	σ_0 [MPa]	G_0 [kJ/m^2]	σ_a [MPa]	G_a [kJ/m^2]
epoxy	5	0.2	20	0.6
MMA	2	0.2	10	2.4

3. Experimental evaluation of integrated PA wires

Typical load-displacement responses, corresponding ERR curves, and fracture surface observations of DCB specimens with three integrated PA wires are shown in Figure 4. Typical curves of DCB specimens with only epoxy adhesive layer (without PA) are also plotted in light grey for comparison. For the DCB specimen without PA, the obtained ERR reaches the peak at nearly 100-mm crack length and then catastrophic brittle fracture happens to the entire joint for an extended debonding. Therefore, no average ERR could be obtained, since no plateau region could be identified in the ERR curve. Severe safety concerns may arise due to such catastrophic brittleness of bonded composite joints, limiting the application of our surface patterning strategy in a thick adhesive layer.

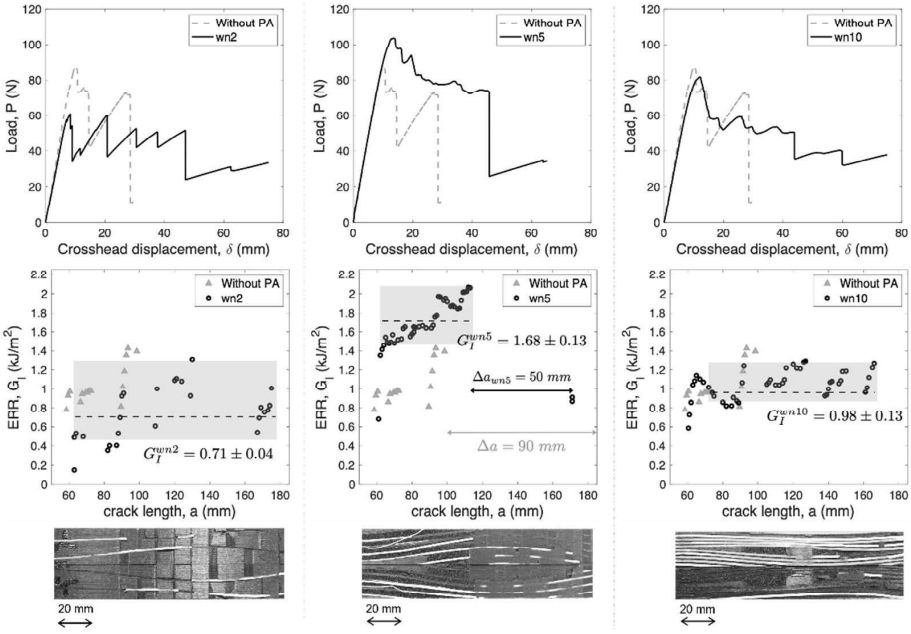

Figure 4. Typical load-displacement responses, corresponding ERR curves, and fracture surfaces of DCB configurations integrated with wn2, wn5, and wn10.

  doi:10.5075/epfl-298799_978-2-9701614-0-0

On the contrary, all specimens with integrated PA wires demonstrate a more stable softening behavior. With only two PA wires integrated within the adhesive layer (wn2), we could see a clear stick-slip load-displacement curve. The plateau of ERR is scattering and a relatively low average value (0.71 kJ/m^2) is obtained by averaging the plateau region in ERR curves of all tested specimens (highlighted by the grey areas in Figure 4). No catastrophic fast crack propagation is viewed compared to that without PA wires. Based on the optical fracture surface, adhesive ligaments were triggered, and PA wires started to hold after the failure of epoxy ligaments. Only two integrated PA wires are not strong enough to further hold the separating arms, which is consistent with the large ERR scattering and relatively low ERR.

When integrating five wires in a DCB specimen (wn5), the obtained ERR is largely enhanced up to 1.68 kJ/m^2. A large load drop is observed in the load-displacement curve of wn5, indicating the presence of an extensive debonding due to the release of stored energy. However, compared to without PA configuration, wn5 demonstrates a higher ERR and a smaller growth of the debonding (50 mm instead of 90 mm in Figure 4), illustrating a better toughening and a more progressive damage. During loading of wn5, large scale bridging of PA wires could be viewed, associated with a large improvement in ERR. Apart from crack jumps at CFRP/epoxy interfaces, fracture surface of wn5 also shows cohesive failure of epoxy. Moreover, bridging PA wires are highly stretched, largely plastic deformed, and finally fractured. Therefore, multiple damage mechanisms are responsible of the enhancement of ERR in this configuration.

Further increasing the number of integrated wires, wn10, could not improve such toughening effect. wn10 only reaches a similar load and ERR level as that without PA, lower than that of wn5. However, its plateau region of ERR is more stable than that of wn2 and exhibits a higher average value of 0.98 kJ/m^2. Besides, the fracture surface illustrates that the main crack propagates at PA/epoxy interfaces, with detached PA wires and cohesive failure of epoxy. Therefore, the alternative surface patterning on CFRP substrates is deactivated in this configuration. The integrated PA wires acted like a carrier within a commercial adhesive film, as already reported in Heide-Jørgensen's work [8].

4. Numerical comparison of brittle and ductile adhesive materials

Simulated load-displacement responses, corresponding ERR curves, and bridging observations of DCB specimens with epoxy adhesive with three thickness values are shown in Figure 5. The locations of arrest interfaces are highlighted in green in the observations. Simulation results show that the adhesive thickness affects the generation of the adhesive ligament, and the bridging of epoxy adhesive ligament is limited. When the thickness is 0.5 mm and 1 mm, the crack jumps from the bottom to the top interface, but the bridging epoxy ligament fractures quickly without a large-scale extrinsic bridging. While 2-mm thick adhesive layer will entirely eliminate the bridging of ligament, and the elevated ERR is due to the detaching from the arrest region G_a. Such observations echoed the limitation of brittle epoxy adhesive, and they also indicate the motivation for embedding PA fibers: to hold the joint after the early failure of the epoxy layer.

As for a more ductile MMA adhesive, simulation showed a distinct behavior. When the thickness is 0.5 mm and 1 mm, a clear extrinsic bridging ligament is generated. Obtained ERR illustrated two increase stages. At the first stage, the crack propagation is arrested by the green arrest interface till the crack jumps from the bottom to the top interface. Different from the epoxy

adhesive, where ERR starts to drop back to the baseline G_0 after the crack jump, MMA adhesive ligament gradually extends the bridging length up to 4 mm, leading to a second rising stage of ERR curve. Therefore, thanks to the plastic energy dissipation, ERR could experience an extra enhancement and further slowdown the crack propagation. In the case of 2-mm thick MMA adhesive layer, the simulation stops before the crack jump due to the convergence issue. If the length of the arrest interface increases to 10 mm, a similar extrinsic bridging ligament as those in 0.5-mm and 1-mm thick adhesive layer is expected. Further work is needed to analyze this relationship and maximize the extrinsic toughening when using the MMA adhesive.

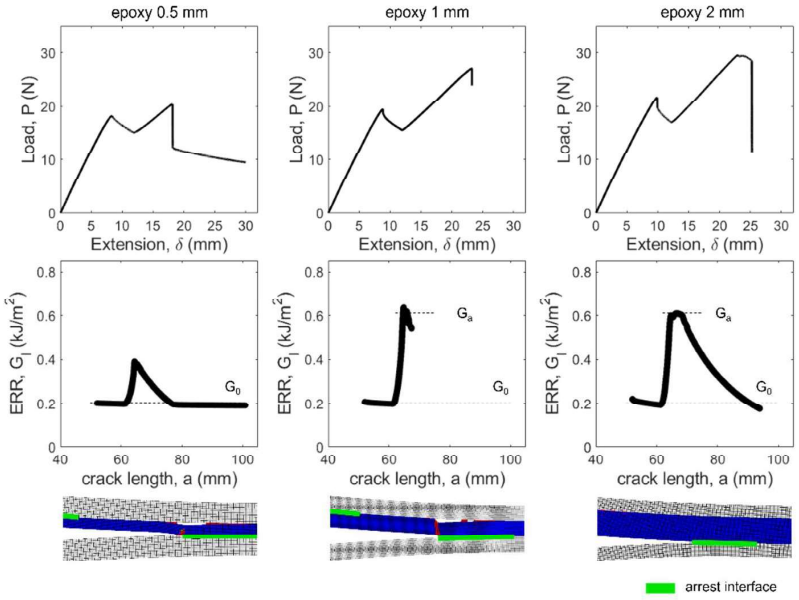

Figure 5. Simulated load-displacement responses, corresponding ERR curves, and bridging observations of DCB with adopted epoxy adhesive with 0.5 mm, 1 mm, and 2 mm thickness.

5. Conclusions

In this work, two methods to further promote ERR and slow down crack propagation of secondary adhesive bonding of CFRP is summarized. The first method is to integrate PA wires within the epoxy adhesive layer. Experimental DCB results indicated that embedded PA wires introduced complex failure mechanisms, softening the joint damage behavior. The second way is to directly adopt a more ductile MMA adhesive material. Numerical investigations showed that, by promoting plasticity, extrinsic bridging could be extended and ERR would be further increased when using MMA instead of epoxy adhesive. Therefore, a more ductile adhesive layer could further improve ERR and stabilize the crack propagation, leading to a toughened and more damage tolerant adhesive joint.

Acknowledgements

The research reported in this publication was supported by funding from both King Abdullah University of Science and Technology (KAUST) Office of Sponsored Research (OSR) under award number OSR-2017-CRG6-3388.01 and Delft University of Technology (TU Delft).

  doi:10.5075/epfl-298799_978-2-9701614-0-0

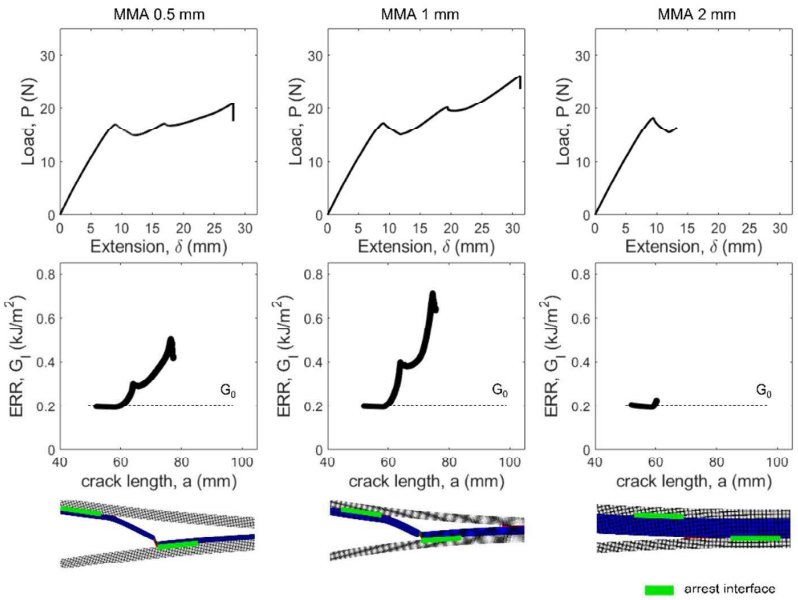

Figure 6. Simulated load-displacement responses, corresponding ERR curves, and bridging observations of DCB with adopted MMA adhesive with 0.5 mm, 1 mm, and 2 mm thickness.

6. References

1. Tao R, Li X, Yudhanto A, Alfano M, Lubineau G. Laser-based interfacial patterning enables toughening of CFRP/epoxy joints through bridging of adhesive ligaments. Composites Part A: Applied Science and Manufacturing 2020; 139:106094.
2. Li X, Lu S, Lubineau G. Snap-back instability of double cantilever beam with bridging. International Journal of Solids and Structures 2021; 233:111150.
3. Saleh MN, Budzik MK, Saeedifar M, Zarouchas D, De Freitas ST. On the influence of the adhesive and the adherend ductility on mode I fracture characterization of thick adhesively-bonded joints. International Journal of Adhesion and Adhesives 2022; 115:103123.
4. Tao R, Alfano M, Lubineau G. Laser-based surface patterning of composite plates for improved secondary adhesive bonding. Composites Part A: Applied Science and Manufacturing 2018; 109:84-94.
5. Yudhanto A, Almulhim M, Kamal F, Tao R, Fatta L, Alfano M, Lubineau G. Enhancement of fracture toughness in secondary bonded CFRP using hybrid thermoplastic/thermoset bondline architecture. Composites Science and Technology 2020; 199:108346.
6. Standard test method for mode I interlaminar fracture toughness of unidirec- tional fiber-reinforced polymer matrix composites, ASTM Internat. 2014.
7. Tao R, Li X, Yudhanto A, Alfano M, Lubineau G. On controlling interfacial heterogeneity to trigger bridging in secondary bonded composite joints: An efficient strategy to introduce crack-arrest features. Composites Science and Technology 2020; 188:107964.
8. Heide-Jørgensen S, de Freitas ST, Budzik MK. On the fracture behaviour of CFRP bonded joints under mode I loading: Effect of supporting carrier and interface contamination. Composites Science and Technology 2018; 160:97-110.

